

then be performed, yielding for the transition rate ($\hbar = 1$)

$$\begin{aligned} \gamma_e(N) = & 2[1 + \bar{n}(\omega_{eg})]\mu_\alpha\mu_\beta \left[\int d^3x |\Phi(\mathbf{x})|^2 \text{Im} G_{\alpha\beta}(\mathbf{x}, \mathbf{x}, \omega_{eg}) \right. \\ & + \int d^3x_1 d^3x_2 \Phi(\mathbf{x}_1)\Phi^*(\mathbf{x}_2) \langle N | \Psi_g^\dagger(\mathbf{x}_1)\Psi_g(\mathbf{x}_2) | N \rangle \\ & \left. \times \text{Im} G_{\alpha\beta}(\mathbf{x}_1, \mathbf{x}_2, \omega_{eg}) \right], \end{aligned} \quad (3)$$

where the excited state is given by the normalized wave function $\Phi(\mathbf{x})$. We denote $\bar{n}(\omega_{eg})$ the average photon number at frequency ω_{eg} in thermal equilibrium. For the sake of simplicity, we restrict ourselves for the rest of the paper to a field at zero temperature where the thermal photon number $\bar{n}(\omega_{eg})$ is negligible. We have expressed the photon propagator through the retarded response (Green) function

$$\begin{aligned} G_{\alpha\beta}(x_1, x_2) = & \int \frac{d\omega}{2\pi} e^{i\omega(t_1-t_2)} G_{\alpha\beta}(\mathbf{x}_1, \mathbf{x}_2, \omega) \\ = & i \langle [E_\alpha(x_1), E_\beta(x_2)] \rangle \Theta(t_1 - t_2). \end{aligned} \quad (4)$$

This quantity is easily calculated in a general environment, for example near a surface, see Ref.[13], and shows oscillating behavior as function of the atom-surface separation.

In eqn. (3), the decay rate naturally splits into a term $\gamma_e^{(0)}$ that remains in the absence of the atom cloud (first line) and an additional term $\gamma_e^{\text{BEC}}(N)$ which describes the bosonic enhancement. The first term has a natural interpretation in terms of an average of local decay rates over the position distribution of the excited state wavepacket. (For a study of the dynamics of the excited state, see Ref.[14].) The analysis of the second term is the main focus of this paper. Note that it depends on the two-point correlation function of the ground state atoms. The bosonic stimulation is thus a probe of the spatial coherence of the Bose gas.

2.2 Discussion of Bose enhancement in free space

To illustrate the physics in eqn. (3), we will assume that both the ground-state BEC and the excited atom are trapped in overlapping isotropic harmonic potentials, far enough away from any macroscopic body. We use the free-space expression $G_{\alpha\beta}^{(0)}$ of the em Green tensor (4) which takes the form

$$G_{\alpha\beta}^{(0)}(\mathbf{x}_1, \mathbf{x}_2, \omega_{eg}) = \int \frac{d^3k}{(2\pi)^3} G_{\alpha\beta}^{(0)}(k, \omega_{eg}) e^{i\mathbf{k}\cdot(\mathbf{x}_1-\mathbf{x}_2)}. \quad (5)$$

As is well known, only photons on the light cone contribute to the imaginary part of this quantity, i.e., $|\mathbf{k}| = \omega_{eg}/c \equiv k_{eg}$. Another relevant length scale is the oscillator length $a_0 = (M\omega_T)^{-1/2}$ of the ground-state trapping potential (M is the atomic mass and ω_T the trap frequency). We assume that the excited-state wave packet $\Phi(\mathbf{x}; \eta)$ is an isotropic Gaussian with a width ηa_0 . The first term in eqn. (3) gives $\gamma_e^{(0)} = \mu^2 k_{eg}^3 / (3\pi\epsilon_0)$, the free space decay rate [13].

Fig. 1 shows how the decay rate $\gamma_e(N)$ varies with the width parameter η , in the presence of a Bose condensate with $N = 10\,000$ Rb atoms (three-dimensional, isotropic trap). We consider both an ideal gas model (solid red lines) and an interacting Bose gas (dash-dotted lines). The upper black

curve corresponds to an ideal gas at zero temperature, where all the ground-state atoms populate the trap ground state $\psi_0(\mathbf{x})$, a gaussian with width a_0 . In this case the integrations in eqn. (3) can be worked out explicitly. We find analytically that the optimum value of $\gamma_e(N)$ is obtained for

$$\eta_{\text{opt}} = \frac{1}{\sqrt{3}} (\sqrt{9 + (k_{eg}a_0)^4} - (k_{eg}a_0)^2)^{1/2}, \quad (0 < \eta_{\text{opt}} < 1). \quad (6)$$

This result as well as the typical behaviour of $\gamma_e(N)$ is easy to understand by noting that the decay rate for a given photon momentum \mathbf{k} is proportional to the overlap integral

$$\int d^3x \Phi(\mathbf{x}, \eta) \psi_{\mathbf{n}}^*(\mathbf{x}) e^{i\mathbf{k}\cdot\mathbf{x}}, \quad (7)$$

where $\mathbf{n} = \mathbf{0}$ for the BEC ground mode. In the so-called Lamb-Dicke limit $k_{eg}a_0 \ll 1$ (well-localized trap), the exponential in eqn. (7) can be approximated by unity, and the overlap is optimal when the two wavepackets are matched in width, $\eta = 1$. The opposite case looks closer to a homogeneous system and is easier to analyze in Fourier space where the photon recoil provides a shift of the momentum distribution. This reduces the overlap and can be compensated for by making an excited-state wave packet wider in momentum space, i.e., $\eta < 1$. At the optimum value, the width is of the order of the photon momentum and the shifted excited-state wave packet still has some overlap with the sharp zero-momentum component of the BEC.

The temperature dependence in Fig. 1 closely follows the occupation of the ground-state (condensate) mode. We have used Ref.[15] where the two-point correlation function $\langle N | \Psi_g^\dagger(\mathbf{x}_1)\Psi_g(\mathbf{x}_2) | N \rangle$ for the ideal Bose gas in a 3D trap is given in a simple form, involving only a single summation. This provides the Bose enhancement of $\gamma_e(N)$ in a straightforward manner for atom temperatures T_A below and above the critical temperature T_c (see caption). We see that for any η , the transition rate drops below the zero-temperature value, and for temperatures above T_c , it becomes comparable to $\gamma_e^{(0)}$ (horizontal dashed line). The temperature dependence is shown in fig. 2, and compared to the condensate fraction N_0/N (dashed line). The bosonic enhancement closely follows the population of the condensate mode because the excited-state wave packet $\Phi(\mathbf{x})$ has the largest overlap with the trap ground state. The thermal occupation of higher lying trap states hence diminishes the integrals eqn. (7). We note that this behaviour would change qualitatively in lower-dimensional systems where the Bose gas occupies excited states with a relatively larger weight.

The more realistic case of an interacting Bose gas is also shown in Fig.1. We focus here on repulsive interactions (corresponding to positive s-wave scattering length a_s), and restrict ourselves to temperatures far below T_c , where it is legitimate to approximate the field operator by the condensate mode only:

$$\langle N | \Psi_g^\dagger(\mathbf{x}_1)\Psi_g(\mathbf{x}_2) | N \rangle \approx N \psi_0^*(\mathbf{x}_1)\psi_0(\mathbf{x}_2). \quad (8)$$

Elementary excitations of the condensate can be included within Bogoliubov theory [16, 17, 18]. The condensate wave function $\psi_0(\mathbf{x})$ is a solution of the Gross-Pitaevskii equation.

We have used the approximate variational solution [19]

$$\bar{\psi}_0(\mathbf{x}) = \frac{c_0(\tau)}{N_0 R^{3/2}} (1 - x^2/R^2)^{(1+\tau)/2} \Theta(R - x), \quad (9)$$

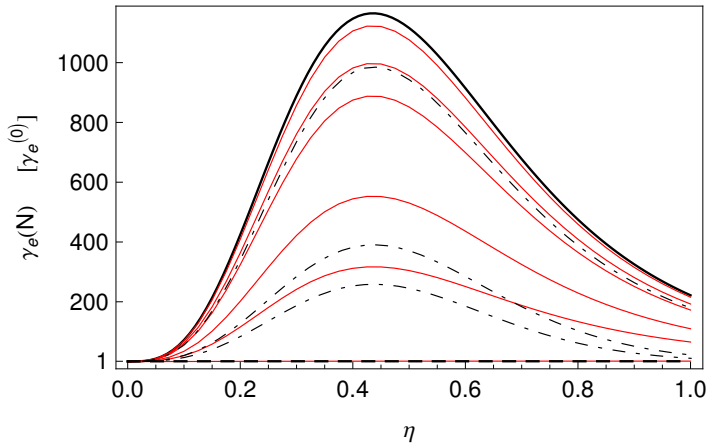


Figure 1: Decay rate of an excited wave packet embedded in a Bose condensate with N atoms. The rate $\gamma_e(N)$ [eqn. (3)] is normalized to the free-space value $\gamma_e^{(0)} = \mu^2 k_{eg}^3 / (3\pi\epsilon_0)$ and plotted as a function of the width ηa_0 of the excited state, scaled to the oscillator length for the BEC trap. The ground-state cloud consists of $N = 10000$ atoms, with trap frequency $\omega_T/2\pi = 1$ kHz (oscillator length $a_0 = 0.34 \mu\text{m}$), the resonance wavelength is $2\pi/k_{eg} = 780$ nm as for rubidium. The optimal value of η [eqn. (6)] is $\eta_{\text{opt}} = 0.44$. *Upper black curve*: ideal Bose gas at zero temperature. *Solid (red) curves*: ideal Bose gas at temperature $T_A = 0.3, 0.5, 0.6, 0.8, 0.9, 1.2 T_c$ with critical temperature $T_c = \omega_T(N/\zeta[3])^{1/3}$ (top to bottom). *Dash-dotted curves*: interacting Bose gas with mode function eqn. (9), for varying s-wave scattering length $a_s = 1, 5, 10 \bar{a}_s$ (top to bottom), with $k_{eg}\bar{a}_s = 0.047$ as for rubidium. *Horizontal dashed line*: free-space decay rate $\gamma_e^{(0)}$.

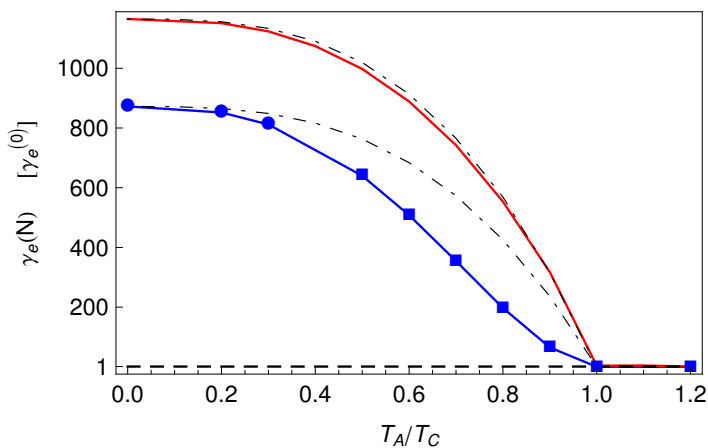


Figure 2: Decay rate and absorption line width vs temperature T_A of an (ideal) Bose gas, for an optimized excited state wave packet. The rate $\gamma_e(N)$ is given in units of the free-space value $\gamma_e^{(0)}$. Trap and atom parameters are the same as in fig. 1. *Red (upper) curve*: decay rate eqn. (3) with $\eta = \eta_{\text{opt}} = 0.44$. *Blue (lower) curve*: line width $\gamma_{\text{abs}}(N)$ [eqn. (17)] of the absorption spectrum. *Dashed-dotted curves*: condensate fraction N_0/N , scaled to the $T = 0$ values. *Horizontal dashed line*: free-space decay rate $\gamma_e^{(0)}$.

that interpolates between a Gaussian and the Thomas-Fermi limit as the parameter $N_0 a_s / a_0$ is changing from zero to infinity. The length R and the exponent τ are fixed by minimizing the Gross-Pitaevskii energy functional, and c_0 is a normalization constant. The result for the decay rate $\gamma_e(N)$ is shown by the dashed-dotted curves in fig. 1, as the interaction parameter $N_0 a_s / a_0$ is increased. Relative to the s-wave scattering length \bar{a}_s of rubidium, we took $a_s = 1, 5, 10 \bar{a}_s$ (top to bottom) which can be achieved using a Feshbach resonance, for example. The interacting gas shows a flatter density profile in the trap, as is well known; this results in smaller values of the overlap integrals eqn. (7).

To summarize the data of Fig.1, we find a relatively strong enhancement of the spontaneous decay rate of an excited atom embedded in a Bose condensate. This happens despite the non-perfect overlap that encodes the constraints of momentum conservation and photon recoil. The optimum conditions correspond to a well-localized excited-state wavepacket (on the scale of the transition wavelength) and a strong condensate fraction ($T \lesssim 0.5 T_c$).

3 Bose enhancement near a surface

In this section, we calculate the transition rate eqn. (3) near a surface and demonstrate its enhancement in a Bose condensate of oblate shape. This scenario can be realized with an optical lattice, by retro-reflecting an off-resonant laser beam at the surface [20], or in a bichromatic evanescent wave [21]. We take the surface in the xy -plane and the trapped atoms centered at a distance d from the surface in the positive z -direction. Concerning the surface material, we use the idealized model of a perfectly reflecting mirror for the sake of simplicity; but with the appropriate choice of (frequency-dependent) reflection coefficients that appear in the photonic Green function $G_{\alpha\beta}(x_1, x_2, \omega)$, a wide range of surface materials can be treated in the same manner[22, 13].

As we have measurements in mind where the control over the distance d is essential, we take an oblate Bose condensate and assume for simplicity a single gaussian mode with widths a_0 (in the xy -plane) and $a_0/\sqrt{\lambda} \ll d$ (along the z -axis). The depletion of the condensate and its broadening due to repulsive interactions could be incorporated as in Sec.2. For the excited state, we adopt again a gaussian wave packet localized in the cloud center, with widths ηa_0 and $\eta_z a_0/\sqrt{\lambda}$, respectively. The actual values of the trap frequency are given in the caption of fig. 3. As the very narrow confinement in the z -direction describes a quasi-2D scenario, the temperature has to be lower than $T_c^{(2D)} = \omega_{\parallel}(N/\zeta[2])^{1/2}$ to ensure a strong condensate occupation.

Fig. 3 illustrates the decay rate $\gamma_e(N)$ obtained from eqn. (3) as a function of the distance d . As is well known, the rate depends on the orientation of the dipole moment (parallel or perpendicular to the surface, represented in red and blue, respectively). The full curves show the Bose-enhanced contribution $\gamma_e^{\text{BEC}}(N, d)$, while the dashed curves give the

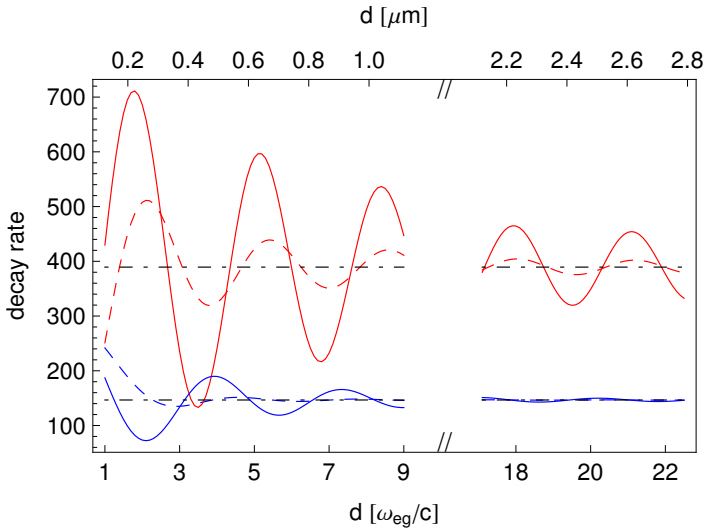


Figure 3: Bose-enhanced decay rate $\gamma_e(N)$ near an interface. The BEC contains 10^5 Rb atoms in an oblate wave function at an average distance d from a perfectly reflecting surface. The size parameters are $a_0 = 3.4 \mu\text{m}$ parallel and $a_0/\sqrt{\lambda} = 0.01 a_0$ perpendicular to the surface, corresponding to trapping frequencies of $\omega_{\parallel}/2\pi = 10\text{Hz}$ and $\omega_{\perp} = 10^4 \omega_{\parallel}$ and a critical temperature $T_c^{(2D)} = 118\text{nK}$. The excited wave packet (resonance frequency as in fig. 1) is spatially centered in the BEC, with size parameters $\eta = 0.07$ and $\eta_z = 1$ relative to a_0 . *Full red curve*: Bose-enhanced decay rate $\gamma_e^{\text{BEC}}(N)$ given by eqn. (3), for an excited atom with its dipole moment oriented parallel to the surface. We normalize to the free-space decay rate $\gamma_e^{(0)}(d \rightarrow \infty)$. *Full blue curve*: $\gamma_e^{\text{BEC}}(N)$ for an excited atom with perpendicular dipole moment. *Horizontal dashed lines*: asymptotic values of $\gamma_e^{\text{BEC}}(N, d \rightarrow \infty)$ at large separation. *Dashed red (blue) curve*: single-atom decay rate $\gamma_e^{(0)}$ (first line of eqn. (3)) for parallel (perpendicular) dipole orientation; these data are multiplied by a factor of 390 and 150, respectively, such that their asymptotic values for large distances d coincide with $\gamma_e^{\text{BEC}}(N)$.

single-atom part $\gamma_e^{(0)}(d)$, re-scaled such that the asymptotic value for large distances d coincides with $\gamma_e^{\text{BEC}}(N, d \rightarrow \infty)$. The numbers given in fig. 3 are the result of a compromise between a tight confinement in the vertical (z -) direction and a localized wave packet in the excited state. The atomic wave packets must be confined below the wavelength in the z -direction, otherwise the oscillations in γ_e vs. distance are averaged out. In this limit, the optimal Bose enhancement is found for an excited wave packet that is matched to the condensate ($\eta_z = 1$). For the size parameter in the xy -plane, we find an optimum at $\eta = 0.07$. The asymptotic values $\gamma_e(N, d \rightarrow \infty)$ are enhanced by factors of 390 and 150 compared to $\gamma_e^{(0)}(d \rightarrow \infty)$ for the parallel and perpendicular dipole, respectively. The difference between these two numbers and the relative phase shift of the oscillation pattern in $\gamma_e^{\text{BEC}}(d)$ are due to the radiation pattern of the dipole emission, combined with the shape of the ground state mode that modulates the Bose enhancement in \mathbf{k} -space.

Fig. 3 thus demonstrates a significant amplification of the decay rate above the surface, with the oscillation amplitude receiving an additional enhancement relative to the asymptotic free-space component. It suggests that even at a distance of a few microns (several transition wavelengths), Bose enhancement can bring the tiny interference structure of the decay rate into an experimentally detectable regime.

4 Virtual excited atoms produced by laser absorption

The calculation above assumed the presence of an excited atom prepared in a gaussian wave packet, and one may ask the question whether this is a realistic description. Indeed, the preparation of such a state would typically proceed by illuminating the system. We therefore describe in this section a calculation of a typical absorption spectrum. We find that the results of the previous section are qualitatively unchanged. The method also illustrates the relevance of two- and four-point correlation functions of the Bose gas. For the sake of simplicity, we restrict this analysis to the ideal Bose gas.

The calculation proceeds by keeping a continuum of modes for the excited state field operator $\Psi_e(x)$ and by identifying the absorption spectrum of a weak laser field with a suitable T -matrix element (self-energy). We take the laser field to be described by a coherent state $|\beta\rangle$ in a given plane-wave mode.

In the leading order of perturbation theory, the absorption by the atom cloud of a photon out of the coherent state $|\beta\rangle$ and re-emitting it into the same state,

$$\begin{array}{c} \beta \quad \beta \\ \swarrow \quad \searrow \\ N \rightarrow \text{---} \rightarrow N \end{array}, \quad (10)$$

results in a (complex) energy shift of the laser plus atom system that is described by the T -matrix element

$$\langle N, \beta | T^{(2)} | N, \beta \rangle = \frac{|\beta|^2 \omega_L}{2} \hat{e}_{\alpha}(\mathbf{k}_L) \hat{e}_{\beta}(\mathbf{k}_L) \frac{N \mu_{\alpha} \mu_{\beta}}{\omega_{eg} - \omega_L - i\epsilon}. \quad (11)$$

In eqn. (11), $|\beta|^2$ is the number of photons in the coherent state, ω_L and \mathbf{k}_L denote the frequency and wave vector of the absorbed photons, the unit vectors $\hat{e}(\mathbf{k}_L)$ denote axes of (linear) photon polarization, and the infinitesimal $\epsilon \searrow 0$ ensures the adiabatic switching-on of the laser field. At this order of perturbation theory, the absorption of photons by the atom cloud is proportional to $\text{Im} \langle N, \beta | T^{(2)} | N, \beta \rangle \propto \delta(\omega_{eg} - \omega_L)$.

The next order in perturbation theory brings about the diagram

$$\begin{array}{c} \beta \quad \beta \\ \swarrow \quad \searrow \\ N \rightarrow \text{---} \rightarrow N \end{array}, \quad (12)$$

which gives the following contribution to the T -matrix:

$$\begin{aligned} \langle N, \beta | T^{(4)} | N, \beta \rangle &= -\frac{|\beta|^2 \omega_L}{2} \hat{e}_{\alpha}(\mathbf{k}_L) \hat{e}_{\beta}(\mathbf{k}_L) \frac{\mu_{\alpha} \mu_{\beta}}{[\omega_{eg} - \omega_L - i\epsilon]^2} \\ &\times \int d^3 x_1 \int d^3 x_2 \langle \Psi_g^{\dagger}(\mathbf{x}_2) \Psi_g(\mathbf{x}_2) \Psi_g^{\dagger}(\mathbf{x}_1) \Psi_g(\mathbf{x}_1) \rangle \\ &\times \mu_{\gamma} \mu_{\delta} G_{\gamma\delta}(\mathbf{x}_1, \mathbf{x}_2, \omega_L) e^{-i\mathbf{k}_L \cdot (\mathbf{x}_1 - \mathbf{x}_2)}. \end{aligned} \quad (13)$$

Let us introduce the density correlation function of the Bose gas as

$$C(\mathbf{x}_2, \mathbf{x}_1) = \langle \Psi_g^{\dagger}(\mathbf{x}_2) \Psi_g(\mathbf{x}_2) \Psi_g^{\dagger}(\mathbf{x}_1) \Psi_g(\mathbf{x}_1) \rangle - n(\mathbf{x}_2) n(\mathbf{x}_1) \quad (14)$$

where $n(\mathbf{x}_1) = \langle \Psi_g^{\dagger}(\mathbf{x}) \Psi_g(\mathbf{x}) \rangle$ is the average density. This splits eqn. (13) in two parts: $\langle T^{(4)} \rangle = \langle T_{\text{scat}}^{(4)} \rangle + \langle T_{\text{abs}}^{(4)} \rangle$. The former contains only densities and can be identified with the

elastic scattering of photons off the inhomogeneous density profile of the BEC. This term does not distinguish between a Bose gas and a classical system with the same density. Its imaginary part provides, by the optical theorem, the total scattering cross section of the BEC. The second term $\langle T_{\text{abs}}^{(4)} \rangle$, on the contrary, is proportional to density fluctuations, and these are at the origin of bosonic enhancement [23, 24]. We therefore identify $\text{Im} \langle T_{\text{abs}}^{(4)} \rangle$ with the change in the atomic absorption spectrum (line width).

Indeed, if we define the resonant part of the polarizability $\alpha_{\alpha\beta}^{\text{res}}(\omega)$ of the atom cloud as

$$\alpha_{\alpha\beta}^{\text{res}}(\omega) = \frac{N\mu_{\alpha}\mu_{\beta}}{\omega_{eg} - \omega - i\epsilon}. \quad (15)$$

we see that the process eqn. (12) can be re-written as a shift of the atomic transition frequency $\omega_{eg} \rightarrow \omega_{eg} + \delta\omega_{eg}$ with

$$\begin{aligned} \langle T^{(2)} \rangle + \langle T_{\text{abs}}^{(4)} \rangle &= \frac{|\beta|^2 \omega_L}{2} \hat{e}_{\alpha}(\mathbf{k}_L) \hat{e}_{\beta}(\mathbf{k}_L) \\ &\times \left[\alpha_{\alpha\beta}^{\text{res}}(\omega_L) + \delta\omega_{eg} \frac{\partial \alpha_{\alpha\beta}^{\text{res}}(\omega_L)}{\partial \omega_{eg}} \right]. \end{aligned} \quad (16)$$

By identifying eqn. (13) and eqn. (16), we can read off the frequency shift $\delta\omega_{eg}$ whose imaginary part yields the atomic line width (the inverse lifetime of the virtual state involving an excited atom)

$$\begin{aligned} \gamma_{\text{abs}}(N) &= -2 \text{Im} \delta\omega_{eg} \\ &= \frac{2}{N} \mu_{\alpha}\mu_{\beta} \left[\int d^3x n(\mathbf{x}) \text{Im} G_{\alpha\beta}(\mathbf{x}, \mathbf{x}, \omega_L) \right. \\ &\quad \left. + \int d^3x_1 \int d^3x_2 C(\mathbf{x}_1, \mathbf{x}_2) \text{Im} G_{\alpha\beta}(\mathbf{x}_1, \mathbf{x}_2, \omega_L) e^{-i\mathbf{k}_L \cdot (\mathbf{x}_1 - \mathbf{x}_2)} \right]. \end{aligned} \quad (17)$$

This function depends weakly on the laser frequency, and we evaluate it at $\omega_L = \omega_{eg}$ for simplicity. We shall use below Wick's theorem to evaluate the density correlation function [25], as appropriate for the ideal Bose gas:

$$C(\mathbf{x}_1, \mathbf{x}_2) = \left| \langle \Psi_g^{\dagger}(\mathbf{x}_2) \Psi_g(\mathbf{x}_1) \rangle \right|^2 \quad (18)$$

Eqs.(17, 18) can now be compared to the decay rate $\gamma_e(N)$ of an excited-state wave packet (eqn. (3)). The first term in both expressions is very similar, and we see that the laser spectroscopy effectively prepares an excited state density profile matched to the condensate density. The second terms differ because the laser wave-vector appears explicitly. Also the one-body density matrix for the excited state, $\langle e | \Psi_e^{\dagger}(x_2) \Psi_e(x_1) | e \rangle$ in eqn. (2), is replaced by its ground-state equivalent $\langle N | \Psi_g^{\dagger}(\mathbf{x}_2) \Psi_g(\mathbf{x}_1) | N \rangle$ in eqn. (17). The prepared wavepacket is hence no longer pure. This makes the temperature dependence of $\gamma_{\text{abs}}(N)$ stronger, as can be seen in Fig.2 (compare the blue and red curves). The calculation of $\gamma_{\text{abs}}(N)$ involves, because of the squared correlation function, a double summation over single-particle trap states [15] under the integral. At zero temperature, the summations can be done analytically, at the low temperatures $T_A = 0.2, 0.3 T_c$, the double sum could be evaluated numerically (circles in fig. 2), while for $T_A/T_c \geq 0.5$, the summations can be accurately replaced by integrations that evaluate faster (denoted

by squares). The size parameter η was set to the optimal value obtained from Fig.1. Although the line width $\gamma_{\text{abs}}(N)$ is for these parameters around 30% smaller than the optimized decay rate $\gamma_e(N)$, the strong Bose enhancement is still working in a qualitatively similar way for both types of processes. We expect a similar result to hold for an absorption experiment near a surface, using for example evanescent fields as discussed in Refs.[26, 27, 28].

5 Summary

To summarize, the presence of a trapped BEC can significantly enhance the decay of an excited atom by bosonic stimulation. The magnitude of the effect depends on the overlap between the atomic wave functions and the wavevector of the photon involved in the decay. More precisely, our calculations based on a quantum field theory of the atom-photon interaction illustrate the importance of two- and four-point correlation functions of the ground-state field for the Bose enhancement. For an excited atom prepared in a Gaussian wavepacket, the transition rate to the ground state can be increased under optimum conditions by a factor $N/10$ where N is the atom number in the BEC. This effect also amplifies the small oscillations of the decay rate near an interface. We have provided an alternative calculation based on the absorption of a laser beam that qualitatively confirms the simpler wave packet picture. The main difference is that absorption from the laser field prepares a non-pure excited state which matches the one-body density matrix of the Bose gas.

Acknowledgement

This work was supported by *Deutsche Forschungsgemeinschaft* (DFG). We thank Dalimil Mazáč for fruitful discussions.

References

- [1] E. A. Hinds, Perturbative cavity quantum electrodynamics, in: P. R. Berman (Ed.), *Cavity Quantum Electrodynamics*, Adv. At. Mol. Opt. Phys., Academic, New York, 1994, p. 30, suppl. 2.
- [2] S. Haroche, Cavity quantum electrodynamics, in: J. Dalibard, J.-M. Raimond, J. Zinn-Justin (Eds.), *Fundamental Systems in Quantum Optics* (Les Houches, Session LIII), North-Holland, Amsterdam, 1992, p. 767.
- [3] V. V. Ivanov, R. A. Cornelussen, H. B. van Linden van den Heuvell, R. J. C. Spreeuw, Observation of modified radiative properties of cold atoms in vacuum near a dielectric surface, *J. Opt. B: Quantum Semiclass. Opt.* 6 (11) (2004) 454.
- [4] J. Javanainen, Optical signatures of a tightly confined Bose condensate, *Phys. Rev. Lett.* 72 (1994) 2375.
- [5] J. J. Hope, C. M. Savage, Stimulated enhancement of cross section by a Bose-Einstein condensate, *Phys. Rev. A* 54 (1996) 3177.
- [6] O. Morice, Y. Castin, J. Dalibard, Refractive index of a dilute Bose gas, *Phys. Rev. A* 51 (1995) 3896.
- [7] A. Görlitz, A. P. Chikkatur, W. Ketterle, Enhancement and suppression of spontaneous emission and light scattering by quantum degeneracy, *Phys. Rev. A* 63 (2001) 041601.
- [8] J. Schiefele, C. Henkel, Bose-Einstein condensate near a surface: Quantum field theory of the Casimir-Polder interaction, *Phys. Rev. A* 82 (2010) 023605.
- [9] G. A. Moreno, D. A. R. Dalvit, E. Calzetta, Bragg spectroscopy for measuring Casimir-Polder interactions with Bose-Einstein condensates above corrugated surfaces, *New J. Phys.* 12 (2010) 033009.

- [10] D. A. R. Dalvit, P. A. M. Neto, A. Lambrecht, S. Reynaud, Probing quantum-vacuum geometrical effects with cold atoms, *Phys. Rev. Lett.* 100 (4) (2008) 040405.
- [11] M. Lewenstein, L. You, J. Cooper, K. Burnett, Quantum field theory of atoms interacting with photons: Foundations, *Phys. Rev. A* 50 (1994) 2207.
- [12] W. Zhang, D. F. Walls, Quantum field theory of interaction of ultracold atoms with a light wave: Bragg scattering in nonlinear atom optics, *Phys. Rev. A* 49 (1994) 3799.
- [13] J. M. Wylie, J. E. Sipe, Quantum electrodynamics near an interface, *Phys. Rev. A* 30 (1984) 1185.
- [14] Y. Japha, V. M. Akulin, G. Kurizki, Atom binding and reflection by spatially inhomogeneous spontaneous emission, *Phys. Rev. Lett.* 80 (17) (1998) 3739.
- [15] S. M. Barnett, S. Franke-Arnold, A. S. Arnold, C. Baxter, Coherence length for a trapped Bose gas, *Journal of Physics B: Atomic, Molecular and Optical Physics* 33 (2000) 4177.
- [16] S. Stringari, Collective excitations of a trapped Bose-condensed gas, *Phys. Rev. Lett.* 77 (12) (1996) 2360.
- [17] B. Hu, G. Huang, Y.-l. Ma, Analytical solutions of the bogoliubov-de gennes equations for excitations of a trapped Bose-Einstein-condensed gas, *Phys. Rev. A* 69 (6) (2004) 063608.
- [18] P. Öhberg, E. L. Surkov, I. Tittonen, S. Stenholm, M. Wilkens, G. V. Shlyapnikov, Low-energy elementary excitations of a trapped Bose-condensed gas, *Phys. Rev. A* 56 (5) (1997) R3346.
- [19] A. Fetter, Variational study of dilute Bose condensate in a harmonic trap, *Journal of Low Temperature Physics* 106 (1997) 643.
- [20] R. J. C. Spreeuw, T. Pfau, U. Janicke, M. Wilkens, Laser-like scheme for atomic-matter waves, *Europhys. Lett.* 32 (1995) 469.
- [21] Y. B. Ovchinnikov, S. V. Shul'ga, V. I. Balykin, An atomic trap based on evanescent light waves, *J. Phys. B* 24 (14) (1991) 3173.
- [22] J. E. Sipe, The dipole antenna problem in surface physics: A new approach, *Surf. Sci.* 105 (1981) 489.
- [23] W. Ketterle, S. Inouye, Does matter wave amplification work for fermions?, *Phys. Rev. Lett.* 86 (19) (2001) 4203.
- [24] M. G. Moore, P. Meystre, Atomic four-wave mixing: Fermions versus bosons, *Phys. Rev. Lett.* 86 (19) (2001) 4199.
- [25] T. S. Evans, D. A. Steer, Wick's theorem at finite temperature, *Nuclear Physics B* 474 (1996) 481.
- [26] J.-Y. Courtois, J.-M. Courty, S. Reynaud, Quantum nondemolition measurements using a crossed Kerr effect between atomic and light fields, *Phys. Rev. A* 52 (1995) 1507.
- [27] A. Aspect, R. Kaiser, N. Vansteenkiste, P. Vignolo, C. I. Westbrook, Non-destructive detection of atoms bouncing on an evanescent wave, *Phys. Rev. A* 52 (1995) 4704.
- [28] R. A. Cornelussen, A. H. van Amerongen, B. T. Wolschrijn, R. J. C. Spreeuw, H. B. van Linden van den Heuvell, Cold trapped atoms detected with evanescent waves, *Eur. Phys. J. D* 21 (3) (2002) 347.